

Productive and nonproductive binding to ribonuclease A: X-ray structure of two complexes with uridylyl(2',5')guanosine

LUIGI VITAGLIANO,¹ ANTONELLO MERLINO,¹ ADRIANA ZAGARI, AND LELIO MAZZARELLA

Centro di Studio di Biocristallografia, CNR, and Dipartimento di Chimica, Università degli Studi di Napoli "Federico II,"
Via Mezzocannone 4, I-80134 Napoli, Italy

(RECEIVED November 16, 1999; FINAL REVISION April 7, 2000; ACCEPTED April 7, 2000)

Abstract

Guanine-containing mono- and dinucleotides bind to the active site of ribonuclease A in a nonproductive mode (retro-binding) (Aguilar CF, Thomas PJ, Mills A, Moss DS, Palmer RA, 1992, *J Mol Biol* 224:265–267). Guanine binds to the highly specific pyrimidine site by forming hydrogen bonds with Thr45 and with the sulfate anion located in the P1 site. To investigate the influence of the anion present in the P1 site on retro-binding, we determined the structure of two new complexes of RNase A with uridylyl(2',5')guanosine obtained by soaking two different forms of pre-grown RNase A crystals. In one case, RNase A was crystallized without removing the sulfate anion strongly bound to the active site; in the other, the protein was first equilibrated with a basic solution to displace the anion from the P1 site. The X-ray structures of the complexes with and without sulfate in P1 were refined using diffraction data up to 1.8 Å (*R*-factor 0.192) and 2.0 Å (*R*-factor 0.178), respectively. The binding mode of the substrate analogue to the protein differs markedly in the two complexes. When the sulfate is located in P1, we observe retro-binding; whereas when the anion is removed from the active site, the uridine is productively bound at the B1 site. In the productive complex, the electron density is very well defined for the uridine moiety, whereas the downstream guanine is disordered. This finding indicates that the interactions of guanine in the B2 site are rather weak and that this site is essentially adenine preferring. In this crystal form, there are two molecules per asymmetric unit, and due to crystal packing, only the active site of one molecule is accessible to the ligand. Thus, in the same crystal we have a ligand-bound and a ligand-free RNase A molecule. The comparison of these two structures furnishes a detailed and reliable picture of the structural alterations induced by the binding of the substrate. These results provide structural information to support the hypotheses on the role of RNase A active site residues that have recently emerged from site-directed mutagenesis studies.

Keywords: protein–inhibitor complex; protein structure–function; retro-binding; ribonuclease; X-ray diffraction

After being the model system for pioneering studies in protein chemistry, bovine pancreatic ribonuclease (RNase A) in the 1980s started to be considered an uninteresting digestive enzyme. This trend has been rapidly reversed by the discovery that several enzymes homologous to RNase A, such as bovine seminal ribonuclease, angiogenin, and onconase, are endowed with a variety of biological functions, including human tumor growth inhibition

(Benner & Allemann, 1989; Youle & D'Alessio, 1997). Several site-directed mutagenesis studies have shown that the ribonucleotidic activity of these enzymes is essential in carrying out these special functions (Youle & D'Alessio, 1997, and references therein). Therefore, the wealth of information collected on the enzymatic properties of RNase A can be fruitfully extended to these important enzymes.

RNase A is an endoribonuclease that cleaves and hydrolyzes single-stranded RNA in two distinct steps (Raines, 1998). In the first step, the imidazolium side chain of His12 acts as a base to extract a proton from the 2'-hydroxyl of the substrate, thus facilitating its attack on phosphorus atom. The His119 side chain acts as an acid to protonate the 5'-oxygen, facilitating its release. In the second step, the enzyme catalyzes the attack on the 2',3'-cyclic phosphodiester by a water molecule, producing a phosphate monoester on C3' of the ribose sugar unit on RNA. Thus, the first step

Reprint requests to: Lelio Mazzarella, Dipartimento di Chimica, Università degli Studi di Napoli "Federico II," Via Mezzocannone 4, I-80134 Napoli, Italy; e-mail: mazzarella@chemna.dichi.unina.it.

¹These authors contributed equally to this work.

Abbreviations: 2',5'-UpG, uridylyl(2',5')guanosine; CSD, Cambridge Structural Database; PDB, Protein Data Bank; RMSD, root-mean-square deviation; RNase, ribonuclease; RNaseA-UpG, complex of RNase A with 2',5'-UpG; sf-RNaseA-UpG, complex of sulfate-free RNase A with 2',5'-UpG.

involves the cleavage of the RNA chain, and the second step involves the hydrolysis of an intermediate product. Catalytically important residues at the RNase A active site were originally identified from studies of the stereochemistry of catalysis (Usher, 1969) and subsequently from low resolution crystallographic analyses of complexes of the enzyme with inhibitors (Richards & Wyckoff, 1973). Recently, high resolution crystallographic analysis and NMR studies have confirmed and expanded these results (Fontecilla-Camps et al., 1994; Zegers et al., 1994; Toiron et al., 1996). These investigations have shown that catalytically important His12 and His119 are located on either side of the phosphate site P1. Lys41 also interacts with the phosphate and it can potentially act as a general base in RNA cleavage (Wladkowsky et al., 1998). The pyrimidine specificity of the enzyme results from the binding of the base in a narrow pocket on the surface of the enzyme (B1 site) formed by Val43, Thr45, Phe120, and Ser123. Each of these residues is conserved in at least 36 of the 41 known amino acid sequences of pancreatic ribonucleases (Beintema et al., 1988). The primary specificity of RNase A is achieved by hydrogen bonding of the substrate with Thr45, which can interact both with uridine and cytidine. Stacking interactions with the Phe120 side chain further stabilizes the binding at the B1 site. A role for Asp83 in the cytidine/uridine specificity of RNase A has been proposed (del-Cardayré & Raines, 1995). Crystallographic studies on oligonucleotides have shown that the downstream adenine base is located in the less specific B2 site constituted by the loop 65–72 containing Asn71, Asn67, and Gln69. The adenine forms two hydrogen bonds with the Asn71 side chain and stacks against the His119 side chain. The presence of additional binding sites, suggested by several biochemical studies, has been shown by Fontecilla-Camps et al. (1994).

Despite this large body of structural studies, further analysis is still required on the interactions of RNase A with the substrate. In particular, the binding of guanine containing mono- and dinucleotides is peculiar. The revision of the structure of RNase A complexes, obtained by soaking pre-grown crystals with cytidylyl(2',5')guanosine and deoxycytidylyl(3',5')guanosine (Aguilar et al., 1991, 1992), revealed that the sulfate anion, which is usually located in P1 in the ligand-free form of the enzyme, is not displaced by the dinucleotides and that the guanine binds at the B1 site through a network of hydrogen bonds with Thr45 and with the anion in P1. The remaining portion of the dinucleotide extends toward the solvent and is partially disordered. This novel type of nonproductive binding has been named retro-binding. Retro-binding occurs also for complexes obtained by cocrystallization (Lisgarten et al., 1995; Vitagliano et al., 1999), thus showing that it is not due to the restrictions imposed when nucleotides are soaked into protein crystals via solvent channels. Although the biological significance of retro-binding is still unclear, it has been shown that its occurrence is not restricted to RNase A. Indeed, retro-binding has been found in other members of the pancreatic-like ribonuclease superfamily (Chang et al., 1998), including bovine seminal ribonuclease, which is endowed with special biological functions (Vitagliano et al., 1999).

To investigate whether retro-binding is affected by the presence of the sulfate ion in the active site, we determined the structure of two new complexes of RNase A with uridylyl(2',5')guanosine by soaking two different crystal forms of the protein. In one case, RNase A was crystallized without removing the sulfate anion bound to the active site, whereas in the other the protein was preliminarily equilibrated with a basic solution to displace the anion from the P1 site.

Results

The structure of RNase A complexed with 2',5'-UpG

The first complex of RNase A with 2',5'-UpG (hereafter referred to as RNaseA-UpG) was prepared by soaking pre-grown monoclinic RNase A crystals, obtained by using untreated protein purchased from Sigma Co. (St. Louis, Missouri) (type XII A). The final model of RNaseA-UpG, which includes 72 water molecules, was refined to an *R*-factor of 0.192 using diffraction data up to 1.8 Å resolution. The average *B*-factor computed for all the nonhydrogen atoms is 17.4 Å² (15.2 and 19.8 Å² for the main-chain and side-chain atoms, respectively). A full list of the refinement statistics of RNaseA-UpG complex is reported in Table 1.

The inspection of the electron density map of the active site provides clear evidence of retro-binding (Fig. 1). In agreement with the findings reported for complexes of RNase A with cytidylyl(2',5')guanosine and deoxycytidylyl(3',5')guanosine (Aguilar et al., 1991), the sulfate anion is placed in P1 and the guanine in B1. In occupying the B1 site, O6 and N7 of the base form hydrogen bonds with the backbone N and O^γ1 of Thr45. N1 and N2 of guanine form two additional hydrogen bonds with two oxygen atoms of the sulfate. The sulfate retains the interactions with the side chains of Gln11, His12, His119, Lys41, and with the backbone nitrogen of Phe120 usually observed when this anion is located in P1 (Gilliland, 1997). The remainder of the dinucleotide extends to the solvent and becomes progressively disordered (Fig. 1). In this complex the 2',5'-UpG adopts an extended conformation with an antiglycoside linkage between the guanine and the ribose. The solvent-exposed sugar ring displays a C2'-exo conformation.

The comparison of RNase A structure in this complex with previously determined structures of RNase A shows that retro-binding does not induce any significant variation on the structure of the protein. The root-mean-square deviations (RMSDs), computed on the backbone atoms, are in the range of 0.14–0.17 Å

Table 1. Refinement statistics

	sf-RNaseA-UpG	sf-RNaseA-UpG
Resolution limits (Å)	8.0–1.8	8.0–2.0
Number of reflections		
with $F > 2\sigma(F)$	10,305	14,101
<i>R</i> -factor ^a	0.192	0.178
Number of protein atoms	951	1,894 ^b
Number of inhibitor atoms	20	21
Number of water molecules	72	97
Number of sulfate anions	1	0
RMSD from ideal values		
Bond lengths (Å)	0.013	0.013
Bond angles (°)	1.85	1.98
Dihedral angles (°)	24.0	23.8
Average <i>B</i> -factors (Å ²)		
Protein atoms	17.4	21.7
Inhibitor atoms	37.1	41.0
Solvent atoms	34.6	30.0

^a R -factor = $\sum |F_o(h) - F_c(h)| / \sum F_o(h)$, where $F_o(h)$ and $F_c(h)$ are the observed and calculated structure factor amplitudes for reflection h .

^bThe side chains of the N-terminal lysines were not included in the final model.

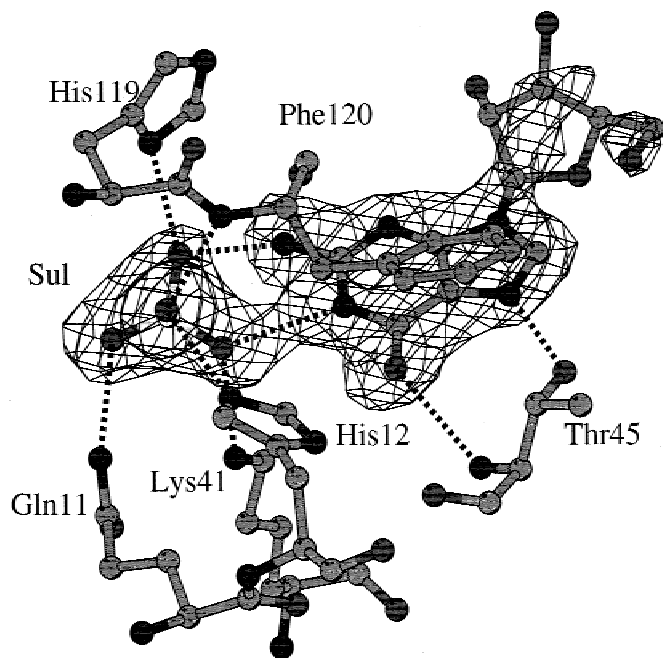


Fig. 1. RNaseA-UpG complex: omit $F_o - F_c$ electron density (contoured at 3.0σ level) of the active site region. The picture was drawn by using BOBSCRIPT (Kraulis, 1991; Esnouf, 1997).

when the protein structure is compared to sulfate-bound RNase A (Wlodawer & Sjölin, 1983) and to RNase A in complexes exhibiting retro-binding (Aguilar et al., 1991; Lisgarten et al., 1995).

The structure of sulfate-free RNase A complexed with 2',5'-UpG

To remove the sulfate anion from the active site of RNase A, the protein was equilibrated against solutions with gradually increasing pH (see Materials and methods). Crystals of the sulfate-free enzyme were obtained by using the conditions reported by Leonidas et al. (1997). In this crystal form, two molecules are present in the asymmetric unit. The complex was obtained by soaking these crystals with 2',5'-UpG. Diffraction data for the complex of sulfate-free RNase A with 2',5'-UpG (hereafter referred to as sf-RNaseA-UpG) were collected at 2.0 Å. The final model of the complex, which includes 97 water molecules, presents an R -factor of 0.178. The average B -factors for all the nonhydrogen atoms of the two molecules are both 21.7 Å². A full list of the refinement statistics of sf-RNaseA-UpG complex is reported in Table 1.

Some interesting features of the active sites of the two molecules in the asymmetric unit were revealed by the inspection of the electron density. In one molecule (hereafter denoted as molecule I), a well-defined electron density was observed for uridine at the B1 site (Fig. 2). In addition, the quality of the electron

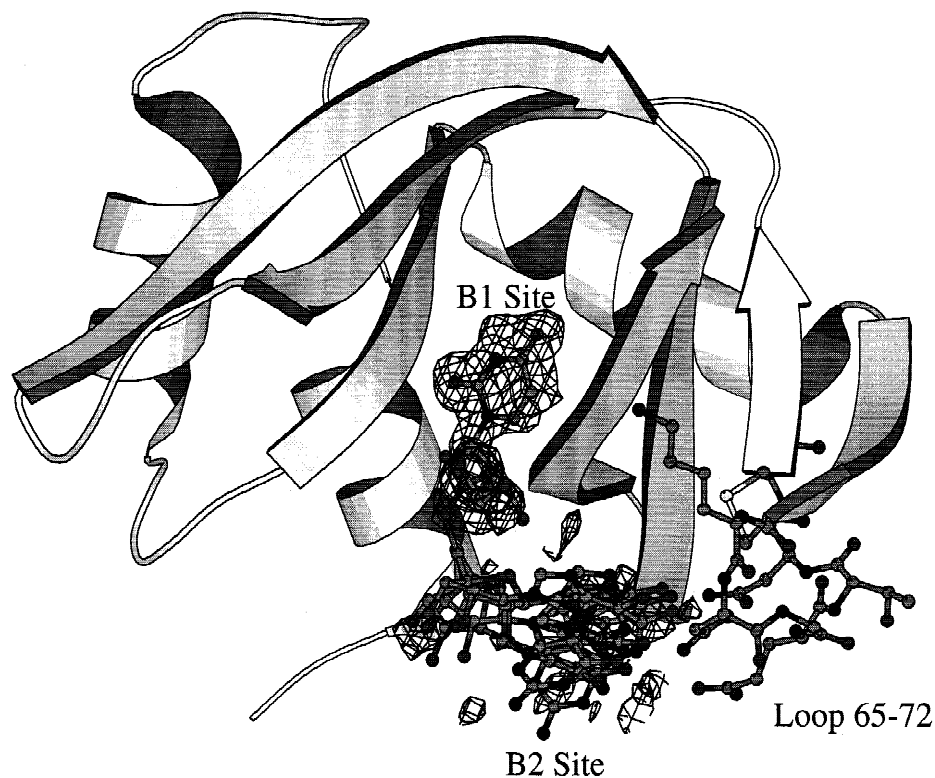


Fig. 2. Sf-RNaseA-UpG complex: omit $F_o - F_c$ electron density (contoured at 2.0σ level) of molecule I active site. Several energetically allowed conformations of the dinucleotide (see text) are also shown.

density allows the positioning for the uridine-linked ribose and the phosphate in P1. By contrast, no electron density is detectable for the guanine base, even though several energetically allowed conformations (Moodie & Thornton, 1993) of the dinucleotide could be located in B2 without any overlap with protein atoms (Fig. 2). Furthermore, there was no evidence of electron density corresponding to a guanine being located in the proximity of Glu111, which according to Tarragona-Fiol et al. (1993) plays a role in the catalytic hydrolysis of CpG. The possibility that 2',5'-UpG could have been cleaved by RNase A during the soaking was also considered. However, chromatographic analysis of the soaking solution containing the enzyme showed that RNase A is unable to hydrolyze the 2',5' dinucleotide, in agreement with previous literature data (Wodak et al., 1977).

A completely different picture emerges from the analysis of the active site electron density of the other molecule (molecule II). In this case, only water molecules are located in the active site (Fig. 3). The analysis of crystal packing reveals that the access of the substrate to this site is partially hindered. As a consequence, there is a ligand-bound and a ligand-free RNase A molecule in the same crystal. The overall structures of molecule I and II are similar. The RMSD computed on backbone atoms of regions with secondary structure is 0.31 Å. Similar deviations are obtained when sulfate-bound (Wlodawer & Sjölin, 1983) and ligand-free (Wlodawer et al., 1988) forms of RNase A are compared.

Detailed description of the active sites of molecules I and II

In molecule I, the interactions of uridine located in the B1 site with the protein (Fig. 4) closely resemble those previously reported

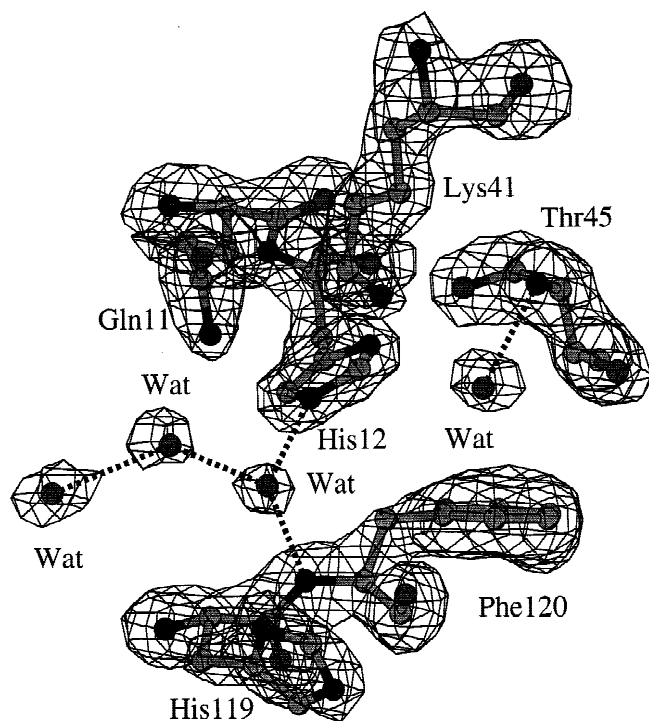


Fig. 3. Sf-RNaseA-UpG complex: omit $F_o - F_c$ electron density (contoured at 3.0σ level) of molecule II active site. The electron density of the catalytically relevant residues is also shown.

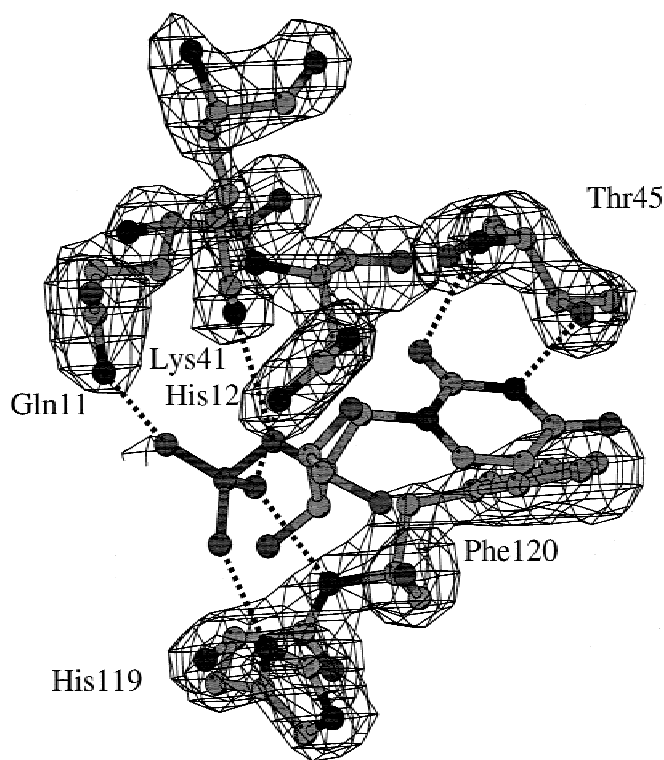


Fig. 4. Sf-RNaseA-UpG complex: interactions of the uridine moiety with the protein residues in molecule I. The electron density (omit $F_o - F_c$ map contoured at 3.0σ level) of the catalytically relevant residues is also shown.

for complexes of RNase A with uridine-containing nucleotides (Wlodawer et al., 1983; Fisher et al., 1998; Wladkowsky et al., 1998). Uridine O2 and N3 form strong hydrogen bonds with N and O γ^1 of Thr45, respectively. As in other complexes of RNase A with uridine-containing nucleotides, O γ^1 of Thr45 is also bound to O δ^1 of Asp83. In addition, two water molecules mediate the interactions of 2',5'-UpG with Asp83 and Ser123 as described by Gililand et al. (1994). The phosphate group is hydrogen bonded to the side chains of His12, His119, Lys41, and Gln11 and to amide nitrogen of Phe120.

The glycosidic linkage between the uridine base and the ribose is anti- and the pseudo-rotation phase angle shows that the sugar ring adopts a C3'-endo pucker. Similar ring puckerings have been reported in the productive bindings of the transition state analog uridine(2',3')cyclic vanadate (Wlodawer et al., 1983; Wladkowsky et al., 1998) and of cytidylic acid (Lisgarten et al., 1993).

In molecule II a cluster of water molecules is located in the active site. The comparison of the active sites of molecules I and II reveals that the binding of the substrate analog displaces two water molecules. The position of these two molecules coincides with two 2',5'-UpG atoms directly bound, via hydrogen bonds, to the protein. In particular, one water molecule is in B1 linked to Thr45 and the other in P1 is strongly linked to Phe120 and His12.

The superimposition of the two active sites also reveals that the binding of the substrate induces small but significant variations in the side-chain orientation for the catalytically important residues Val43, Lys41, Gln11, and His119 (Fig. 5). To establish stronger van der Waals interactions with the pyrimidine base, a rotation of Val43 side chain occurs (Fig. 5A). Furthermore, N ζ of Lys41

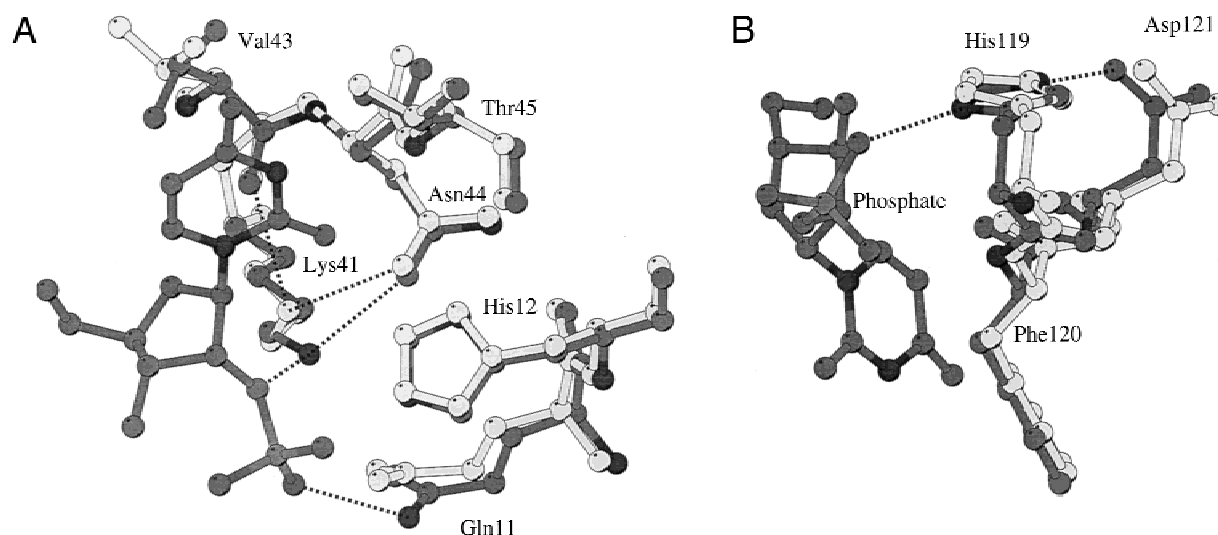


Fig. 5. Sf-RNaseA-UpG complex: superimposition of the active site regions of molecules I and II (light gray). In ball-and-stick representation along with the substrate analog are shown Lys41, Val43, Thr45, His12, Gln11 (A), His119 and Asp121 (B).

changes its hydrogen-bonding contacts. Indeed, while in the ligand-free molecule, it interacts with Val43 O and Asn44 O^{δ1}, in molecule I the Lys41 side chain contributes to the binding of the phosphate moiety while preserving the hydrogen bond with Asn44. In agreement with previous reports (Wlodawer et al., 1988), a rearrangement of the Gln11 side-chain conformation is also observed. It is worth noting that in the ligand-free molecule, this Gln11 side chain is closer to the P1 site than in the ligand-bound molecule, where this residue is hydrogen bonded to the phosphate moiety. Finally, some degrees of flexibility are shown by His119 (Fig. 5B). Several reports in the literature (Gilliland, 1997, and references therein) have demonstrated that this residue can adopt two distinct conformations, usually denoted as A (*trans*) and B (*gauche*). Although in both molecules I and II the His119 side chain adopts the same A rotameric state, its orientation changes slightly. In the ligand-bound molecule, a tilt of the imidazolium ring occurs to optimally bind both the phosphate and Asp121 side chain. It is interesting to note that the distance between O^{δ1} of Asp121 and N^{e2} of His119 is significantly shorter in molecule I (2.8 Å) than in molecule II (3.2 Å).

Interactions of guanine with sulfate and phosphate in small molecules

The structures reported here on RNaseA-UpG and sf-RNaseA-UpG demonstrate the role the sulfate-guanine interaction plays in the occurrence of retro-binding. To further characterize this interaction, we searched for small molecule crystal structures containing both a guanine and sulfate anion in the Cambridge Structural Database (CSD) (Allen et al., 1979). In this search, we found only two structures (CSD codes DEGXA0 and MGCUS) fulfilling this requirement and, interestingly, in both cases sulfate and guanine are linked by two hydrogen bonds as observed in RNaseA-UpG as well as in the other RNase complexes with guanine-containing nucleotides (Aguilar et al., 1992; Lisgarten et al., 1995; Chang et al., 1998; Vitagliano et al., 1999). A similar search was repeated looking for structures containing guanine and the monoanionic

phosphate of nucleotides. In this case, 48 structures were found, and in 18 cases the phosphate is directly bound to the guanine. In four structures, the geometry of this interaction is practically identical to that observed in retro-binding. Other anions, such as nitrate and perchlorate, can establish similar interactions with guanine and can therefore potentially favor retro-binding when bound to RNase A.

Discussion

Several structural studies have revealed that guanine-containing oligonucleotides bind to ribonucleases in a nonproductive way (Aguilar et al., 1991, 1992; Lisgarten et al., 1995; Vitagliano et al., 1999), with the guanine strongly bound to the pyrimidine-specific B1 site (retro-binding). These studies have also shown that the sulfate anion present in P1 forms two strong hydrogen bonds with guanine when retro-binding occurs. To clarify the role of the anion in retro-binding, we determined the structure of two new complexes of RNase A with 2',5'-UpG, soaking two different crystal forms of the protein with the substrate analog. In one case, the protein was crystallized leaving the sulfate in P1, whereas in the other the anion was removed from the active site. The comparison of the 2',5'-UpG binding in the two structures provides clear evidence that the guanine-sulfate interaction is the driving force behind the occurrence of retro-binding. The strength of this interaction also suggests that removal of the sulfate from the active site is a necessary prerequisite to carrying out structural studies on RNase A complexes with guanine-containing nucleotides.

The tendency of guanine to bind the sulfate is also confirmed by a search in the small molecule CSD. Indeed, the interaction is also found in the only two available crystal structures containing both molecules. Furthermore, this survey also shows that the monoanionic phosphate can similarly bind to the guanine. This is particularly interesting, considering the phosphate anion is biologically relevant. This observation suggests that retro-binding can occur also in physiological conditions, and therefore the phosphate anion can exert a selective inhibition against the degradation of small

fragment of RNA containing guanine. However, with the present data, it is not possible to establish whether this inhibition is an evolutionary designed property of RNase A or whether it is merely a minor and undesired feature due to the intrinsic architecture of RNase A active site. It is worth noting that the involvement of the guanine-phosphate interaction in important biological processes has already been proposed. NMR studies on nucleosides (Lancelot & Helene, 1984) have indeed shown that the phosphate anion binds to N1 and N2 of the guanine in a manner that perfectly mimics the sulfate-guanine interaction observed in retro-binding. Moreover, it was found that this interaction is one order of magnitude stronger than the guanine-cytosine interaction in the Watson and Crick base pairing. On the basis of these results, the authors suggested that this interaction might contribute to the formation of a specific secondary structure for RNA-guanine complexes.

The structure of sulfate-free RNase A complexed with 2',5'-UpG represents the first productive complex of a guanine-containing oligonucleotide to RNase A. The uridine and phosphate moieties of the substrate analog bind to the active site by means of a hydrogen bonding network that has been well characterized in previous complexes (Gilliland, 1997). It is worth mentioning that the electron density of the phosphate is not particularly well defined. The *B*-factors of the phosphate group atoms are, indeed, around 50 Å², a value that is comparable to the average *B*-factor of the sugar atoms but much larger than the average *B*-factor of uridine atoms (25 Å²). No electron density has been detected for the downstream guanine base, either in proximity of the loop 65-72, which participates in the binding of the adenine (Zegers et al., 1994; Vitagliano et al., 1998), or in the region of Glu111, which has been suggested to play a role in the catalytic action against CpG (Tarragona-Fiol et al., 1993). This suggests that the purine base does not form specific interactions with the protein in the crystal state. The modeling of the guanine in the active site shows that the base can adopt several energetically allowed conformations without overlapping with any protein atom.

Our findings do not exclude the possibility that weak interactions between the guanine and protein may occur in solution, also considering that loop 65-72 in this crystal form is involved in packing contacts with a symmetry-related molecule. In other words, the intermolecular contacts can decrease the flexibility of the loop and, thus, its ability to bind the substrate analog. This is in line with the results obtained by soaking the same crystals used to prepare sf-RNaseA-UpG with uridylyl(2'-5')adenosine (Mazzarella et al., unpubl. results). In this case, the crystals readily developed cracks, which precluded any possibility of collecting diffraction data. This indicates that the specific link of adenine to the B2 site requires some rearrangements of the loop that are not compatible with crystal packing. On the other hand, the much smaller crystal damage produced by the soaking of 2',5'-UpG indicates that the B2 site has a significantly reduced affinity toward guanine.

In light of these results, we can interpret the different kinetic parameters of RNase A toward UpA and UpG (Kato et al., 1986). It has been reported that the binding affinity of RNase A toward the two substrates does not vary greatly, with K_m for UpG that is only twice the K_m for UpA. On the other hand, k_{cat} toward UpA is almost 40 times k_{cat} for UpG. These data can be explained by assuming that the binding affinity is mainly driven by the hydrogen-bonding network formed by the uridine at the B1 site. This is reasonable considering that the B1 site is located in a rigid region

of the protein whereas B2 is constituted by a rather flexible external loop. As the same interactions at B1 are present in both substrates, similar K_m values are expected. The additional interactions of the adenine at the B2 site may account for the smaller value of K_m measured for UpA. Interestingly, the comparison of the k_{cat} for UpG and UpA indicates that the binding of the adenine at B2 plays a crucial role in the correct positioning of the phosphate in P1. In other words, the binding of the adenine in B2 is not essential for the binding of the substrate, which is nevertheless assured by the binding of the pyrimidine at B1, but it favors the transphosphorylation reaction by directing the appropriate orientation of the phosphodiester linkage in the active site. The absence of a specific interaction of the guanine with the B2 site is, thus, responsible for the low value of k_{cat} found for UpG.

An unusual feature of the sf-RNaseA-UpG complex is that the substrate analog binds to only one of the two molecules present in the asymmetric unit. Thus, the comparison of these two structures represents an ideal opportunity to unveil the structural modifications induced by the substrate. Structural alterations on the RNase A structure produced by the binding of the sulfate in P1 have been previously reported (Campbell & Petsko, 1987; Wlodawer et al., 1988). However, these analyses were carried out comparing sulfate-bound and ligand-free RNase A structures derived from different crystals. This limitation can lead to artifacts and controversial results. As an example, the analysis carried out by Campbell and Petsko (1987) on the overall *B*-factors of the sulfate-bound and ligand-free RNase A structures suggested that the binding of the sulfate increases the overall rigidity of the protein structure. This result was not confirmed by the study of Wlodawer et al. (1988). In sf-RNaseA-UpG, the overall *B*-factors of the ligand-free and ligand-bound molecules are both 21.7 Å². As very similar *B*-factors for the two ligand-free molecules were found in isomorphous crystals (Leonidas et al., 1997), we can confidently conclude that the binding of the substrate analog does not produce a significant variation in the enzyme overall rigidity.

Another controversial aspect regards the possibility that long-range structural alterations can be produced by ligand binding to RNase A (Wlodawer et al., 1988). Comparing structures derived from different crystals, Wlodawer et al. (1988) noticed that in sulfate-bound and ligand-free structures the side chain of the Gln101, a residue that is distant from the active site, adopts two completely different conformations. We have recently shown that the orientation of Gln101 side chain is pH dependent (Berisio et al., 1999). In the molecule I and II of sf-RNaseA-UpG, the Gln101 side chain exhibits the same orientation, thus indicating that the binding at P1 does not influence the Gln101 rotameric state.

The comparison of the molecule I and II active sites provides interesting information on the reorganization of RNase A active site residues upon the binding. This is particularly interesting as these residues have recently been the subject of extensive site-directed mutagenesis studies (Raines, 1998, and references therein). In agreement with several previous reports, our comparison confirms that the B1 site is particularly rigid. The structure of Thr45, which strongly binds the pyrimidine base, is virtually independent of the presence of the substrate in the active site. A small conformational change is shown by the Val43 side chain that is involved in van der Waals interactions with the pyrimidine base.

On the other hand, the residues involved in phosphate binding at P1 site display a larger conformational freedom. Indeed, with the sole exception of His12 (whose side chain is hydrogen bonded to

Thr45), the positions of Lys41, Gln11, and His119 side chains are significantly different in molecules I and II. N^ε of Lys41, which is bound to O of Val43 in molecule II, moves toward the phosphate when the binding occurs. In both cases, however, Lys41 is also hydrogen bonded to the Asn44 side chain. This may suggest that the highly conserved residue Asn44 (Beintema et al., 1988) is important for keeping the charged Lys41 side chain in proximity to the other positively charged residues of RNase A active site. In this way, Lys41 can readily exert its catalytic role.

More intriguing is the conformational variation exhibited by the Gln11 side chain. Superimposing the active site of molecules I and II, it emerges that the conformation adopted by this residue in the ligand-free molecule is not compatible with presence of a phosphate group in P1. Indeed, the distance of Gln11 N^{e2} from an oxygen atom of the phosphate would be <2.0 Å. This findings are in agreement with the kinetic data on Gln11 mutants. Raines and coworkers (delCardayré et al., 1995) showed that replacing the glutamine with an alanine significantly reduces both K_m and k_{cat} , thus suggesting that the presence of Gln11 increases the free energy of the enzyme–substrate complex. This is not surprising, considering that the side chain of this residue partially obstructs the P1 site. On the other hand, the hydrogen bond of Gln11 side chain with the phosphate can contribute to the correct positioning of the phosphodiester group that is cleaved during catalysis, thus increasing the catalytic constant of RNase A. Therefore, as pointed out by Raines (1998), the presence of Gln11 side chain increases the free energy of the Michaelis complex but also prevents nonproductive bindings of the substrate to the RNase A active site.

Finally, the interaction between the side chains of His119 and Asp121 deserves some comments. It is interesting that the His...Asp interaction is strongly stabilized by the presence of the phosphate in P1. Indeed, the rather high distance (3.2 Å) between His119 N^{e2} and Asp121 O^{δ1} suggests that this bond is not particularly strong in the ligand-free form. Only when His119 also binds the substrate, such a contact becomes substantially stronger. In agreement with Schultz et al. (1998), these data indicate that the His...Asp cannot be considered as a low-barrier hydrogen bond, and it cannot play the role that it plays in serine proteases.

Materials and methods

Crystallization and data collection of RNaseA-UpG

Bovine pancreatic ribonuclease purchased from Sigma Chemical Co. (St. Louis, Missouri) (type XII A) was crystallized without further purification by free interface diffusion at 20 °C using 50% 2-methyl-2-propanol as the precipitating agent (Berisio et al., 1999). Monoclinic crystals suitable for X-ray diffraction studies were obtained within three weeks. The complex was obtained by soaking these crystals in a solution containing 60% 2-methyl-2-propanol and 2',5'-UpG at 8 mM concentration for 24 h. The soaking produced cracks on the crystal surface that did not prevent data collection. Only one crystal was used for data collection.

Diffraction data were registered at room temperature to a resolution limit of 1.80 Å on a Nonius Dip 2030b imaging plate. A Nonius FR591 rotating anode, operating at 45 kV and 90 mA, generated CuK α radiation used for data collection. The data were processed using the program suite Denzo and Scalepack (Otwinoski & Minor, 1997). Crystal data and data collection statistics are given in Table 2.

Table 2. Crystal data and data collection statistics

	RNaseA-UpG	sf-RNaseA-UpG
Crystal data		
Space group	P2 ₁	C2
Cell parameters		
<i>a</i> (Å)	30.34	101.44
<i>b</i> (Å)	38.35	33.45
<i>c</i> (Å)	53.85	73.11
β (°)	106.8	90.5
Data collection		
Resolution limits (Å)	15.0–1.8	15.0–2.0
Number of observations	60,998	37,174
Number of unique reflections	10,866	15,833
Completeness (%)	96.4	92.2
R_{sym} ^a (%)	6.8	8.2

^a $R_{sym} = \sum |I(h_i) - \langle I(h) \rangle| / \sum \langle I(h_i) \rangle$, where $I(h_i)$ is the scaled intensity of the i^{th} symmetry-related observation of reflection h and $I(h)$ is the mean value.

Refinement of RNaseA-UpG

The structure of the complex was solved by difference Fourier methods using the high resolution structure of RNase A (PDB code 7RSA) determined by Wlodawer et al. (1988) at 1.26 Å resolution as a starting model. Refinements were carried out using X-PLOR (Brünger, 1992). Refinement cycles were followed by manual intervention, using the molecular graphic program O (Jones et al., 1991) to correct minor errors in position of the side chains and to build missing parts of the model. The stereochemistry of the model was monitored by using PROCHECK (Laskowski et al., 1993). The initial model, which did not include water molecules, showed an *R*-factor of 0.25 using reflections in the 8–2.5 Å resolution range. The electron density maps corresponding to the active site region showed a well-ordered tetrahedral distribution of density in the P1 site and a very flat region of density located at the B1 site that were interpreted as a sulfate anion and a guanine base, respectively. The introduction of these ligands lowered the *R*-factor of the model to 0.23. The inspection of the new difference maps revealed presence of electron density corresponding to the guanine-linked sugar. Water molecule sites were identified and included in the model in subsequent refinements. The final model, which includes 72 water molecules, presents an *R*-factor of $R = 0.192$ using diffraction data with $F > 2\sigma(F)$ in the 8.0–1.8 Å resolution range. Refinement statistics are reported in Table 1.

Crystallization and data collection of sf-RNaseA-UpG

The removal of the sulfate from the RNase A active site was achieved by increasing the pH of the protein solution. RNase A (type XII A from Sigma) was dissolved and equilibrated against solutions with increasing pH. In the final step, the protein solution was dialyzed against a TRIS/HCl at pH 9 for three days. Afterward, the pH was adjusted to 5.5, adding HCl 1 M. Crystallization trials using 2-methyl-2-propanol as the precipitant did not produce good quality crystals. Better results were obtained by using PEG4000 according to the procedure described by Leonidas et al. (1997). Crystals were grown by the hanging drop vapor diffusion at 20 °C. A drop, containing 10 mg/mL protein in 10 mM sodium citrate

buffer pH 5.0 and 10% PEG 4000, was equilibrated against reservoir containing 20% PEG4000 and 20 mM sodium citrate buffer pH 5.0. Crystals grew in about one week. The complex was obtained by soaking these crystals in a solution containing 8 mM 2',5'-UpG, 20 mM sodium citrate buffer (pH 5.0), and 25% PEG4000. Attempts to cocrystallize the complex failed. Diffraction data were collected at 2.0 Å, using the same equipment described above. Statistics of data processing are reported in Table 2.

Refinement of sf-RNase A-UpG

The structure of the complex was solved by difference Fourier methods using the RNase A structure (PDB code 1AFU), determined by Leonidas et al. (1997) at 2.0 Å resolution, as a starting model. The initial refinement of the model showed an *R*-factor of 0.25. The inspection of the electron density maps corresponding to the active sites of the two molecules in the asymmetric unit revealed productive binding of the substrate analog only in one active site. The well-defined electron density of the uridine at B1 demonstrated the occurrence of productive binding. The downstream sugar and phosphate were also visible in the electron density maps. No electron density was detected for the second ribose and the guanine. In the active site of the other molecule, a cluster of water molecules was identified. The final model presents an *R*-factor of 0.179 using diffraction data with $F > 2\sigma F$ in the resolution range. Statistics and parameters of the refinement are shown in Table 1.

Atomic coordinates of RNaseA-UpG and sf-RNaseA-UpG have been deposited in the PDB with entry codes 1EOW and 1EOS, respectively.

Searches in the Cambridge Structural Database

The occurrence of specific interactions of guanine with phosphate and sulfate was analyzed carrying out a survey in the small molecule database CSD. The current version of the database contains more than 190,000 crystal structures. The search was performed using the program QUEST (Allen et al., 1979), selecting structures with an *R*-factor <0.06.

Acknowledgments

The first two authors contributed equally to this work. The authors are indebted to G. Sorrentino, M. Amendola, and P. Occorsio for technical collaboration, and to L. De Luca for help with some of the computations. This work was financially supported by the Agenzia Spaziale Italiana (ASI) and by CNR "PF Biotecnologie."

References

- Aguilar CF, Thomas PJ, Mills A, Moss DS, Palmer RA. 1992. Newly observed binding mode in pancreatic ribonuclease. *J Mol Biol* 224:265–267.
- Aguilar CF, Thomas PJ, Moss DS, Mills A, Palmer RA. 1991. Novel non-productively bound ribonuclease inhibitor complexes—High resolution X-ray refinement studies on the binding of RNase-A to cytidyl-2',5'-guanosine (2',5'-CpG) and deoxycytidyl-3',5'-guanosine (3',5'-dCpG). *Biochim Biophys Acta* 1118:6–20.
- Allen FH, Bellard S, Brice MD, Cartwright BA, Doubleday A, Higgs H, Hummelink T, Hummelink-Peters BG, Kennard O, Motherwell WDS, et al. 1979. The Cambridge Crystallographic Data Centre: Computer-based search, retrieval, analysis and display of information. *Acta Crystallogr B* 35:2331–2339.
- Beintema JJ, Schuller C, Irie M, Carsana A. 1988. Molecular evolution of the ribonuclease superfamily. *Prog Biophys Mol Biol* 51:165–192.

- Benner SA, Allemann RK. 1989. The return of pancreatic ribonucleases. *Trends Biochem Sci* 14:396–397.
- Berisio R, Lamzin VS, Sica F, Wilson KS, Zagari A, Mazzarella L. 1999. Protein titration in the crystal state. *J Mol Biol* 292:845–854.
- Brünger AT. 1992. *X-PLOR v3.1 user's guide. A system for X-ray crystallography and NMR*. New Haven, Connecticut: Yale University Press.
- Campbell RL, Petsko GA. 1987. Ribonuclease structure and catalysis: Crystal structure of sulfate-free native ribonuclease A at 1.5 Å resolution. *Biochemistry* 26:8579–8584.
- Chang CF, Chen C, Chen YC, Hom K, Huang RF, Huang TH. 1998. The solution structure of a cytotoxic ribonuclease from the oocytes of *Rana catesbeiana* (bullfrog). *J Mol Biol* 283:231–244.
- delCardayré SB, Raines RT. 1995. A residue to residue hydrogen bond mediates the nucleotide specificity of ribonuclease A. *J Mol Biol* 252:328–336.
- delCardayré SB, Ribo M, Yokel EM, Quirk DJ, Rutter WJ, Raines RT. 1995. Engineering ribonuclease A: Production, purification and characterization of wild-type enzyme and mutants at Gln11. *Protein Eng* 8:261–273.
- Esnouf RM. 1997. An extensively modified version of MolScript that includes greatly enhanced coloring capabilities. *J Mol Graph* 15:132–134.
- Fisher BM, Schultz LW, Raines RT. 1998. Coulombic effects of remote subsites on the active site of ribonuclease A. *Biochemistry* 37:17386–17401.
- Fontecilla-Camps JC, de Llorens R, Du MHL, Cuchillo CM. 1994. Crystal structure of ribonuclease A d(ApTpApApG) complex. *J Biol Chem* 269:21526–21531.
- Gilliland GL. 1997. Crystallographic studies of ribonuclease complexes. In: D'Alessio G, Riordan JF, eds. *Ribonucleases: Structures and functions*. New York: Academic Press. pp 306–341.
- Gilliland GL, Dill J, Pechik L, Svensson LA, Sjölin L. 1994. The active site of bovine pancreatic ribonuclease: An example of solvent modulated specificity. *Protein Pept Lett* 1:60–65.
- Jones TA, Zou J-Y, Cowan SW, Kjeldgaard M. 1991. Improved methods for building protein models in electron-density maps and the location of errors in these models. *Acta Crystallogr A* 47:110–119.
- Katoh H, Yoshinaga M, Yanagita T, Ohgi K, Irie M, Beintema JJ, Meinsma D. 1986. Kinetic studies on turtle pancreatic ribonuclease: A comparative study of the base specificities of the B2 and P0 sites of bovine pancreatic ribonuclease A and turtle pancreatic ribonuclease. *Biochim Biophys Acta* 873:367–371.
- Kraulis PJ. 1991. MOLSCRIPT: A program to produce both detailed and schematic plots of protein structures. *J Appl Crystallogr* 24:946–950.
- Lancelot G, Helene C. 1984. Phosphate-guanosine interactions. *J Biol Chem* 259:15046–15050.
- Laskowski RA, MacArthur MW, Moss DS, Thornton JM. 1993. PROCHECK: A program to check the stereochemical quality of protein structure. *J Appl Crystallogr* 26:283–291.
- Leonidas DD, Shapiro R, Irons LI, Russo N, Acharya KR. 1997. Crystal structures of ribonuclease A complexes with 5'-diphosphoadenosine 3'-phosphate and 5'-diphosphoadenosine 2'-phosphate at 1.7 Å resolution. *Biochemistry* 36:5578–5588.
- Lisgarten JN, Gupta V, Maes D, Wyns L, Zegers I, Palmer RA, Dealwus CG, Aguilar CF, Hemmings AM. 1993. Structure of the crystalline complex of cytidylic acid (2'-CMP) with ribonuclease at 1.6 Å resolution. Conservation of solvent site in RNase A at high-resolution structures. *Acta Crystallogr D* 49:541–547.
- Lisgarten JN, Maes D, Wyns L, Aguilar CF, Palmer R. 1995. Structure of the crystalline complex of deoxycytidyl-3',5'-guanosine (3',5'-dCpG) cocrystallized with ribonuclease at 1.9 Å resolution. *Acta Crystallogr D* 51:767–771.
- Moodie SL, Thornton JM. 1993. A study into the effects of protein binding on nucleotide conformation. *Nucleic Acid Res* 21:1369–1380.
- Otwinoski Z, Minor W. 1997. Processing X-ray diffraction data collected in oscillation mode. *Methods Enzymol* 276:307–326.
- Raines TA. 1998. Ribonuclease A. *Chem Rev* 98:1045–1066.
- Richards FM, Wyckoff HW. 1973. Ribonuclease S. In: Philips DC, Richards FM, eds. *Atlas of molecular structures in biology*, vol. I. Oxford, UK: Cladron.
- Schultz LW, Quirk DJ, Raines RT. 1998. His...Asp catalytic dyad of ribonuclease A: Structure and function of the wild-type, D121N, and D121A enzymes. *Biochemistry* 37:8886–8898.
- Tarragona-Fiol A, Eggelte HJ, Harbron S, Sanchez E, Taylorson CJ, Ward JM, Rabin BR. 1993. Identification by site-directed mutagenesis of amino acids in the B2 subsite of bovine pancreatic ribonuclease A. *Protein Eng* 6:901–906.
- Toiron C, Gonzalez C, Bruix M, Rico M. 1996. Three-dimensional structure of the complex of ribonuclease A with 2',5'-CpA and 3',5'-d(CpA) in aqueous solution, as obtained by NMR and restrained molecular dynamics. *Protein Sci* 5:1633–1647.
- Usher DA. 1969. On the mechanism of ribonuclease action. *Proc Natl Acad Sci USA* 62:661–667.
- Vitagliano L, Adinolfi S, Riccio A, Sica F, Zagari A, Mazzarella L. 1998.

- Binding of a substrate analog to a domain swapping protein: X-ray structure of the complex of bovine seminal ribonuclease with uridylyl(2'-5')adenosine. *Protein Sci* 7:1691-1699.
- Vitagliano L, Adinolfi S, Sica F, Merlino A, Zagari A, Mazzeola L. 1999. A potential allosteric subsite generated by domain swapping in bovine seminal ribonuclease. *J Mol Biol* 293:566-577.
- Wladkowsky BD, Svensson LA, Sjölin L, Ladner JE, Gilliland GL. 1998. Structure (1.3 Å) and charge state of a ribonuclease A-vanadate complex: Implications for the phosphate ester hydrolysis mechanism. *J Am Chem Soc* 120:5488-5498.
- Wlodawer A, Miller M, Sjölin L. 1983. Active site of RNase: Neutron diffraction study of a complex with uridine vanadate, a transition-state analogue. *Proc Natl Acad Sci USA* 80:3628-3631.
- Wlodawer A, Sjölin L. 1983. Application of joint neutron and X-ray refinement to the investigation of the structure of ribonuclease A at 2.0 Å resolution. *Biochemistry* 22:2720-2728.
- Wlodawer A, Svensson LA, Sjölin L, Gilliland GL. 1988. Structure of phosphate-free ribonuclease A refined at 1.26 Å. *Biochemistry* 27:2705-2717.
- Wodak SY, Liu MY, Wyckoff HW. 1977. The structure of cytidilyl(2',5')adenosine when bound to pancreatic ribonuclease S. *J Mol Biol* 116:855-875.
- Youle RJ, D'Alessio G. 1997. Antitumor RNases. In: D'Alessio G, Riordan JF, eds. *Ribonucleases: Structures and functions*. New York: Academic Press. pp 491-514.
- Zegers I, Maes D, Dao-Thi M-H, Poortmans F, Palmer R, Wyns L. 1994. The structures of RNase A complexed with 3'-CMP and d(CpA): Active site conformation and conserved water molecules. *Protein Sci* 3:2322-2339.